

**This is the accepted manuscript version of the contribution published as:**

**Birkigt, J., Stumpp, C., Małoszewski, P., Nijenhuis, I. (2018):**

[Evaluation of the hydrological flow paths in a gravel bed filter modeling a horizontal subsurface flow wetland by using a multi-tracer experiment](#)

*Sci. Total Environ.* **621** , 265 – 272

**The publisher's version is available at:**

<http://dx.doi.org/10.1016/j.scitotenv.2017.11.217>

1 **Evaluation of the hydrological flow paths in a gravel bed filter modelling a horizontal**  
2 **subsurface flow wetland by using a multi-tracer experiment**

3

4 **Jan Birkigt<sup>1</sup>, Christine Stumpp<sup>2</sup>, Piotr Maloszewski<sup>2,3,†</sup>, and Ivonne Nijenhuis<sup>1\*</sup>**

5 <sup>1</sup>Helmholtz Centre for Environmental Research - UFZ – Department of Isotope

6 Biogeochemistry, Permoserstraße 15, D-04318 Leipzig, Germany

7

8 <sup>2</sup>Helmholtz Zentrum München, German Research Center for Environmental Health – Institute

9 of Groundwater Ecology, Ingolstädter Landstraße 1, D-85764 Neuherberg, Germany

10

11 <sup>3</sup>AGH University of Science and Technology Kraków, Department of Hydrogeology and

12 Engineering Geology, Al. Mickiewicza 30, 30-059 Kraków, Poland

13 <sup>†</sup>Deceased 21 March 2017

14 **\*Corresponding author:**

15 **Ivonne Nijenhuis**

16 **Tel:** +49 341 235 13 56

17 **E-mail:** [ivonne.nijenhuis@ufz.de](mailto:ivonne.nijenhuis@ufz.de)

18

19 **Keywords:** constructed wetland, multi tracer test, mathematical modelling,

20

21 **Abstract**

22 In recent years, constructed wetland systems have become into focus as means of cost-  
23 efficient organic contaminant management. Wetland systems provide a highly reactive  
24 environment in which several removal pathways of organic chemicals may be present at the  
25 same time; however, specific elimination processes and hydraulic conditions are usually  
26 separately investigated and thus not fully understood. The flow system in a three dimensional  
27 pilot-scale horizontal subsurface constructed wetland was investigated applying a multi-tracer  
28 test combined with a mathematical model to evaluate the flow and transport processes. The  
29 results indicate the existence of a multiple flow system with two distinct flow paths through  
30 the gravel bed and a preferential flow at the bottom transporting 68% of tracer mass resulting  
31 from the inflow design of the model wetland system. There the removal of main contaminant  
32 chlorobenzene was up to 52% based on different calculation approaches. Determined  
33 retention times in the range of 22 d to 32.5 d the wetland has a heterogeneous flow pattern.  
34 Differences between simulated and measured concentrations in the upper sediment indicate  
35 diffusion dominated processes due to stagnant water zones. The tracer study combining  
36 experimental evaluation with mathematical modeling demonstrated the complexity of flow  
37 and transport processes in the constructed wetlands which need to be taken into account  
38 during interpretation of the determining attenuation processes.

39

## 40 **1. Introduction**

41 Constructed wetlands have become of increasing interest in recent years as an economical  
42 solution for treating wastewater. Subsurface flow constructed wetlands provide a  
43 heterogeneous filter and buffer system where abiotic and biotic processes, e.g. sorption,  
44 hydrolysis, photolysis, evaporation and biodegradation, may take place simultaneously,  
45 resulting in contaminant removal (Imfeld et al., 2009). Wetlands have been shown efficient in  
46 the removal of organic contaminants such as the chlorinated solvents, pharmaceuticals,  
47 personal health care products, pesticides as well as the immobilization of metals (Gambrell,  
48 1994; Imfeld et al., 2009; Kidmose et al., 2010; Li et al., 2014; Onesios et al., 2009; Schmidt  
49 et al., 2014; Verlicchi and Zambello, 2014). However, the processes contributing to the  
50 removal are not fully understood and of high interest for future wetland applications. The  
51 currently developed applications for industrial and urban scale water treatment, however,  
52 require a detailed understanding of the intertwined processes occurring in the highly  
53 heterogeneous environment of wetland systems (Imfeld et al., 2009). In particular, a thorough  
54 understanding of the water flow characteristics determining the retention time and flow paths  
55 will be a requisite to run such systems efficiently (Zahraeifard and Deng, 2011) and before  
56 up-scaling of these approaches can be successful. Then the implementation can be considered  
57 as feasible alternative or supplement for conventional wastewater treatment or contaminated  
58 site management (Gearheart et al., 1989).

59 To date, several studies were published addressing constructed wetland processes in more  
60 detail. For example, the contributing processes to chloroethene (Imfeld et al., 2010),  
61 monochlorobenzene (Braeckevelt et al., 2007; Schmidt et al., 2014) as well as MTBE  
62 (Jechalke et al., 2010; Rakoczy et al., 2011), pharmaceuticals (Matamoros and Bayona, 2006)  
63 or metals (Weis and Weis, 2004) removal and immobilization and related microbial biomass  
64 (Tietz et al., 2007; Truu et al., 2009) was described (Imfeld et al., 2009). However, these  
65 processes also need an insight into the hydrology and the flow characteristics of such wetland

66 systems (King et al., 1997; Machate et al., 1997; Małozzewski et al., 2006a; Małozzewski et  
67 al., 2006b; Ranieri et al., 2011). Indeed, the understanding of the flow characteristics in a  
68 wetland is of utmost importance for determining the overall residence time of the water in the  
69 system and thus the contact time between the reactive surfaces and contaminant of interest  
70 (Małozzewski et al., 2006b). Overall, the residence time of a contaminant in a treatment  
71 system needs to be longer to the time required for its degradation to reach a complete  
72 removal. Often, only the average residence time is determined as only samples at a single  
73 point without depth distinction within the gravel bed or at the outlet are considered in  
74 constructed wetlands (Guo et al., 2017; Małozzewski et al., 2006b; Ranieri et al., 2011). The  
75 theoretical retention time can be approximated as the ratio between pore water volume within  
76 the bed and the applied volumetric flow rate assuming homogeneous and plug flow conditions  
77 and that all water in the wetland is mobile. In reality, no such homogeneous systems exist and  
78 not only average residence times are of importance but the residence time distributions (RTD)  
79 covering the entire range of potential reaction times. Particularly heterogeneities like  
80 preferential flow or stagnant water zones are of importance as they decrease or increase the  
81 residence time, respectively. In surface water dominated wetlands (Holland et al., 2004;  
82 Lange et al., 2011) as well as in subsurface flow systems (Kidmose et al., 2010; Langergraber,  
83 2008; Małozzewski et al., 2006b), the combined use of tracers and mathematical modeling  
84 have been adequate tools to identify and quantify heterogeneous flow paths and residence  
85 times which can be different from theoretical calculations. Most of these tracer applications  
86 measure the tracer breakthrough curves (BTCs) only at the outlet. The contribution of  
87 different process towards removal, e.g. aerobic, anaerobic or abiotic, are not clear as such  
88 systems are from high complexity in their flow path due to changes in flow,  
89 evapotranspiration, rain gains, heterogeneous distribution of plants, of load and so on which  
90 make each system almost unique (Imfeld et al., 2009). Therefore, the objective of this study  
91 was to identify complex horizontal and vertical transport processes in a constructed wetland.

92 Specifically, we aimed to use a combined multiple tracer and mathematical modelling  
93 approach to quantify different flow paths, transport processes and residence times within the  
94 constructed wetland. The outcome of this study will contribute to a general understanding of  
95 heterogeneous hydrological conditions in similar systems which are crucial to understand  
96 observed removal of contaminants. As a model system, a constructed wetland fed with  
97 monochlorobenzene (MCB) contaminated groundwater was used, consisting of a planted and  
98 unplanted segment (Schmidt et al., 2014). For this study, only the unplanted segment was  
99 investigated. In the unplanted gravel bed filter of this horizontal subsurface-flow constructed  
100 wetland system, about 40% of the MCB was removed in the gravel bed while over the  
101 transition zone into the pond another 50% was eliminated leading to an overall reduction of  
102 MCB of 90% compared to the inflow. The removal was apparently linked to iron reduction,  
103 however, due to the uncertainties in flow paths and actual residence time, the rate of removal  
104 and active regions could not be assessed.

105

## 106 **2. Material and methods**

### 107 **2.1 Model constructed wetland system**

108 The horizontal subsurface flow wetland system within the SAFIRA project located directly at  
109 the contaminated field site in Bitterfeld, Germany consisted of a stainless steel basin with the  
110 dimension of 6 m (length) x 1 m (width) x 0.7 m (depth) (Figure 1) with a gravel bed (5 m x 1  
111 m x 0.6 m) and a free water pond (1 m x 1 m x 0.5 m) at the outflow side (Figure S1 – S3)  
112 (Kaschl et al., 2005; Schmidt et al., 2014). The grain size grading of the filter material was  
113 assessed following standard test DIN 18123 resulting in Gaussian distribution of the granular  
114 size between 0.63 mm and 6.3 mm. Total measured porosity was 41% ( $\epsilon = 0.41$ ). The water  
115 flow was generated through external pumps at the inflow and outflow. Inflow was continuous  
116 using a rotary piston pump from Ismatec (Wertheim, Germany) with a flow rate ( $q$ ) held at 1

117 L h<sup>-1</sup> representative for the conditions in the aquifer corresponding to a hydraulic loading rate  
118 (HLR) of the subsurface flow gravel bed and free water pond of 4.8 mm d<sup>-1</sup> and 24 mm d<sup>-1</sup>,  
119 respectively (Kadlec and Wallace, 2008). The water level at the outflow was held constant at  
120 50 cm (10 cm under gravel bed surface) using a tubing pump from Ismatec (Wertheim,  
121 Germany) controlled by a float sensor from Kobold Messring (Hofheim, Germany). Water  
122 flow mass balances during the tracer test were calculated from the pump rates.

123

## 124 **2.2 Tracer test**

125 A multi tracer test was performed from April to May 2011 (16.3°C mean air temperature).  
126 The gravel bed was covered with polyethylene foil to minimize processes like evaporation,  
127 dilution through rain or photodegradation of the tracer chemicals. A mixture of bromide (as  
128 KBr; 550 mg L<sup>-1</sup>), uranine (120 µg L<sup>-1</sup>) and deuterium oxide (0.14 at%; δD = 8050‰) in  
129 contaminated groundwater from the regional aquifer was injected. Three tracers were chosen  
130 which had different diffusion coefficients, thus allowing identifying stagnant water zones and  
131 diffusion dominated transport processes (Knorr et al., 2016). The tracers were added as a  
132 pulse injection over 20 hours at the flux of 1 L h<sup>-1</sup> from a separate tank which was connected  
133 to the inflow of the wetland. Afterwards, the inflow was reconnected directly to the  
134 groundwater feed keeping the same flow conditions. Samples were taken at 4 m and, as  
135 indicated, at 4.5 m from the inflow central in the gravel bed at three different depths (-27.5  
136 cm; -37.5 cm; -47.5 cm from water surface level) simultaneously with a peristaltic pump from  
137 Ismatec (Wertheim, Germany) at a relatively low flow rate of 4 mL min<sup>-1</sup> to minimize  
138 artificial influences to the flow. Polyethylene scintillation vials from VWR (Darmstadt,  
139 Germany) were filled with 20 mL pore water for each sampling point and time and were  
140 stored in 8 °C temperature in the dark prior to analysis. The sampling regime is listed in  
141 details in SI.

142

### 143 **2.3 Analysis of the tracer chemicals**

144 Bromide concentrations were determined using an ion chromatography from Dionex-Thermo  
145 Scientific (Bremen, Germany) set up with Ion Pac pre-column and analytical column Ion Pac  
146 AS 11-HC (4 x 50 mm; 4 x 250 mm) from Dionex-Thermo Scientific (Bremen, Germany)  
147 with an analytical uncertainty of 0.05 mg L<sup>-1</sup>. Uranine concentrations were measured using a  
148 fluorescence photometer from Taurus Instruments (Weimar, Germany) in a daylight-darkened  
149 laboratory using a non-UV lamp, to avoid errors caused by photodegradation processes during  
150 analysis. Deuterium analyses were done using a high temperature pyrolysis from HEKAtech  
151 (Wegeberg, Germany) coupled to an isotope ratio mass spectrometry from Thermo Scientific  
152 (Bremen, Germany) (HTP-IRMS) with an analytical uncertainty of 0.44‰ (Gehre and  
153 Strauch, 2003).

154 Concentration corrections of the applied tracers were done based on background analyses of  
155 the groundwater. Bromide was below detection limit ( $c_{Br} < 0.5 \text{ mg L}^{-1}$ ), deuterium present at  
156 natural abundance  $\delta D = -69 \pm 1\text{‰}$  and uranine was corrected considering natural fluorescence  
157 of the groundwater (equal to  $c_{Uranine} = 0.176 \pm 0.002 \text{ } \mu\text{g L}^{-1}$ ).

158

### 159 **2.4 Mathematical model**

160 In the present pilot system, the tracer migration can be considered as dispersive-convective  
161 transport within several flow-paths, which meet in the observation port, when considering that  
162 (1) injection takes place in several inflow pipes equally distributed horizontally, resulting in  
163 the transversal line injection close to the bottom of the wetland; (2) transversal vertical  
164 dispersion is small and can be neglected; and (3) the flow conditions are in steady state.  
165 Depending on the results of the tracer breakthrough curves, an appropriate model approach  
166 has to be chosen. Due to similarities in BTCs compared to the previous study by Małoszewski  
167 et al., 2006 (Małoszewski et al., 2006b), investigating the flow paths in artificial wetlands, the

178 Multi-Flow Dispersion Model (MFDM) was chosen. The MFDM model assumes that the  
 179 tracer transport between the inlet to the wetland (injection site) and the observation site (flow  
 180 distance  $x$ ) can be estimated by a combination of singular 1-D dispersion-convection  
 181 equations. Each flow-path is characterized by a specific volumetric flow rate ( $q_i$ ), mean transit  
 182 time of water ( $t_{oi} = v_i/x$ ) or velocity ( $v_i$ ), and longitudinal dispersivity ( $\alpha_{Li}$ ) or dispersion  
 183 parameter ( $P_{Di} = \alpha_{Li}/x$ ). It is assumed that there is no interaction between the flow paths and  
 184 that the whole injected mass of tracer is divided into several flow-paths proportionally to the  
 185 respective volumetric flow rates ( $q_i$ ). The transport of an ideal tracer along  $i^{\text{th}}$  flow-path is  
 186 described by the following equation:

$$177 \quad \alpha_{Li} v_i \frac{\partial^2 C_i}{\partial x^2} + v_i \frac{\partial C_i}{\partial x} = \frac{\partial C_i}{\partial t} \quad (1)$$

178 where  $C_i(t)$  is the concentration of tracer in the effluent from the  $i^{\text{th}}$  flow-path. The solution to  
 179 (1) for a pulse injection was given e.g. in (Hendry et al., 1999; Stumpff et al., 2009) and has  
 180 the following form:

$$181 \quad C_i(t) = C_0 \int_0^t g_i(\tau) d\tau \quad \text{for} \quad t \leq t_{pulse}$$

$$182 \quad C_i(t) = C_0 \int_{t-t_{pulse}}^t g_i(\tau) d\tau \quad \text{for} \quad t > t_{pulse} \quad (2)$$

182 where  $C_0$  is the concentration of tracer in the pulse injection,  $t_{pulse}$  is duration of the pulse and  
 183 the function  $g_i(\tau)$  is equal to:

$$184 \quad g_i(\tau) = \frac{1}{t_{oi} \sqrt{4\pi (P_{Di})_i (\tau/t_{oi})^3}} \cdot \exp \left[ -\frac{(1 - \tau/t_{oi})^2}{4(P_{Di})_i (\tau/t_{oi})} \right] \quad (3)$$

185

186 Mean transit time for the flow-system between injection site and detection port (being in  
 187 different depths “j”) is the flux weighted mean described by the following equation:

$$188 \quad (t_o)_{j \text{ mean}} = \sum_{i=1}^N p_i \cdot (t_o)_i = \frac{V_j}{q_j} \quad (4)$$

189 Where  $V_j$  is the active volume of water between injection and detection port and  $q_j$  is the  
 190 water flux through the volume  $V_j$  observed in different depths (“j”), and  $N$  is the number of  
 191 flow-paths, which has to be found in modeling procedure applied for each depth “j”, and

$$192 \quad p_i = \frac{\int_0^{\infty} C_i(t)_{\text{port}} dt}{\int_0^{\infty} C(t)_{\text{port}} dt} \quad (5)$$

193 where  $C(t)_{\text{port}}$  is the whole concentration curve measured in the water at the observation port  
 194 and  $C_i(t)_{\text{port}}$  is the partial measured concentration curve, resulting at the port from the tracer  
 195 transport within the  $i$ -the flow-path, which must be found by modelling procedure.

196 When the flow rate at the observation port ( $q_j$ ) is known or can be estimated, the volume of  
 197 water in the wetland layer between injection site and observation port ( $V_j$ ) can be calculated  
 198 as:

$$199 \quad V_j = \sum_{i=1}^N V_i \quad (6)$$

200 where

$$201 \quad V_i = p_i \cdot t_{oi} \cdot q_j \quad (7)$$

202 and  $j$  corresponds to upper, middle and lower port. The fluxes  $q_j$  was finally found from the  
 203 surfaces under the whole tracer curve modelled for each depth by adopting equation 5.



## 205 **3. Results**

### 206 **3.1 Tracer experiment**

207 All three tracers, bromide, deuterium oxide and uranine, were detected at all three sampling  
208 depths at the sampling point at 4 m (Figure 2). The highest concentrations of all tracers were  
209 observed at the lowest level (Figure 2c). Here, two main partial breakthrough curves were  
210 detected for all tracers, after approximately 300 and 510 hours, respectively. Interestingly, the  
211 observed second peak with up to 18.4% of the initial concentration was relatively higher  
212 compared to the first peak with up to 9.7%. A third, minor, breakthrough curve was observed  
213 after approx. 800 hours.

214 At the upper levels, bromine and deuterium behaved similarly, different from uranine.  
215 Bromine and deuterium had one main breakthrough peak at approximately 550 hours at the  
216 middle level (Figure 2b) and two peaks at approximately 400 and 720 hours at the upper level  
217 (Figure 2a). Surprisingly, uranine did not have a clear breakthrough curve at the middle and  
218 upper level. Following an increase after approximately 600 and 750 hours at the middle and  
219 upper level, respectively, uranine remained at a low but relatively constant concentration over  
220 the time frame of the experiment.

221 While the maximum concentration was up to 18.4% in the lower level, maximum  
222 concentrations in the middle and upper level were only 3.7% and 3.2%, respectively, of the  
223 initial concentration (Figure 2). Even though the two tracer breakthrough curves in the upper  
224 level arrived around 100 and 200 hours later than in the lower level, respectively, they  
225 followed the same trend transporting more tracer mass in the second curve as compared to the  
226 first curve. However, contrastingly, the only main BTC in the middle level arrived 250 hours  
227 later than in the lower level.

228 Comparing the tracers, D<sub>2</sub>O generally had the highest relative concentrations in the  
229 breakthrough curves, followed by bromine. Uranine generally behaved similar, although with  
230 lower relatively concentrations, in the lower level, however behaved quite differently from  
231 D<sub>2</sub>O and bromine in the middle and upper level, likely due to higher interactions with the  
232 sediment (Davis et al., 1980).

233

### 234 **3.2 Mathematical Modeling**

235 The mathematical multi-flow dispersion model was used to model the breakthrough curves of  
236 the different levels. Exemplary bromide was chosen to discuss the results of the modeling  
237 (Figure 3). The fitted model curves using the MFDM for the other two tracers are shown in SI  
238 (Figure S4, S5). Resulting modeling parameters are summarized in Table 1. The measured  
239 data were well reproduced by the chosen MFDM indicating the presence of complex, multiple  
240 flow paths in the system. The modeling confirmed the preferred flow along the bottom  
241 (lower) layer with 65-70% of mass flowing along the bottom and 14-18% and 16-17% of  
242 mass at the middle and upper level, respectively (Table 2). Highest flow fractions were found  
243 for the second partial BTC in the lower and upper levels, respectively, and for the first partial  
244 BTC in the middle layer. Fitting parameters were similar for deuterium and bromide for all  
245 BTCs in all levels (Table 1). BTCs of uranine resulted in similar transport parameters in the  
246 main flow paths (lower layer), but transport in the middle and upper level were different  
247 indicating a retardation and non-conservative transport behavior of uranine in these layers;  
248 therefore, no results are presented in Table 2 for uranine. Due to a larger mass fraction of  
249 uranine in the third partial BTC at the upper level, also retardation of uranine was found here  
250 despite similarities of individual transit times. Weighted mean transit times were shortest in  
251 the lower level ranging between 21.4 and 22.6 d (see Table 1). Transit times were longer for  
252 the middle and upper level resulting in weighted mean transit times of 28.9 and 31.1 d, and

253 32.3 and 33.9 d for deuterium and bromide, respectively. Dispersivities varied within one  
254 order of magnitude (0.5-8.3 cm). Dispersivities for bromide and deuterium were similar  
255 except for the last BTC in all levels; here, bromide resulted in larger dispersivities compared  
256 to deuterium (see Table 1). Mean transit times found as an average for deuterium and bromide  
257 varied between 22.0 to 32.5 d for lower and upper layer, respectively (see Table 2). Table 2  
258 also shows resulting mean calculated water flux  $q_j$  assuming that the tracer distribution  
259 observed in each level is representative for the horizontal plain in that level. It was the largest  
260 in the lower level ( $0.68q$ ) while in middle and upper levels it was similar and equal to  $0.16q$   
261 (see Table 2). Taking into account that  $q = 1 \text{ L h}^{-1}$  and a total pore water volume of  $0.82 \text{ m}^3$  it  
262 yields to an active pore water volume of  $0.61 \text{ m}^3$  in the lower part of the wetland which  
263 corresponds to effective porosity being approximately 40%.

264

## 265 **4. Discussion**

### 266 **4.1 Flowpath and residence times**

267 The resulting BTCs and transport parameters showed, in contrast to findings of Headley and  
268 colleagues (Headley et al., 2005), that flow and transport in our pilot constructed wetland was  
269 complex and heterogeneous, both in vertical and horizontal direction. The highest  
270 concentrations of all tracers were observed at the lowest level (Figure 2c) suggesting a main  
271 flow path along the bottom of the wetland. Here, two main and one minor, partial  
272 breakthrough curves were detected for all tracers, indicating multiple flow paths at the lower  
273 level. All three tracers showed similar BTC distributions without any pronounced differences  
274 in the tailing of the concentration curves. Consequently, diffusion in this lower level seems to  
275 be negligible. Interestingly, the observations implied the higher mass of tracer transported  
276 through the second main flow path. On the one hand, the heterogeneity can results from not

277 fully mixed conditions between injection and sampling ports along the main flow direction.  
278 Hence, the first BTC at the lower level likely represented water flowing from the middle  
279 injection port to the sampling point and the second peak with higher mass recovery then  
280 resulted from water originating from the two outer injection points. The third BTC could have  
281 been the consequence of water mixed with less mobile water between injection ports (Kadlec  
282 and Wallace, 2008). On the other hand, the different flow paths in the lower level can result  
283 from multiple porous sediment developed from settled organic material resulting in multiple  
284 BTCs like found for heterogeneous aquifers (Vanderborght and Vereecken, 2002).

285 A non-uniform flow through the wetland is obvious when looking at the vertical distribution  
286 of BTCs. First, the mass of the tracer is not equally distributed within the wetland (Tab. 2).  
287 Second, transit times and distributions of BTCs at the middle and upper level were similar but  
288 rather different from the lower level. The sampling procedure itself -due to pumping- is  
289 expected to not substantially influence the tracer migration because the pump rate ( $0.24 \text{ L h}^{-1}$ )  
290 was only one fourth of the total flux ( $1 \text{ L h}^{-1}$ ) through the wetland. From total flux and  
291 assuming uniform flow, a mean flow velocity and transit time of  $0.16 \text{ m d}^{-1}$  and 25 d could be  
292 estimated, respectively.

293

#### 294 **4.2 Differences between tracers**

295 Comparing the used tracers, deuterium can be considered as an ideal tracer of water sources  
296 and movements (Kendall and McDonnell, 1999). Minor difference in relative concentrations  
297 (Fig. 2) between deuterium and bromide can be explained either by analytical uncertainties,  
298 which are relatively higher for bromide compared to deuterium, or by anion properties of  
299 bromide. Bromide has been reported to be affected by sorption or anion exclusion under  
300 specific conditions (Gilley et al., 1990; Korom, 2000; Levy and Chambers, 1987) and on plant

301 uptake especially in wetlands (Whitmer et al., 2000). The latter is irrelevant because the  
302 wetland was unplanted.

303 Substantial differences were found for uranine compared to the other two tracers. Most  
304 notable was the different transport behavior of uranine with the initial absence and delayed  
305 occurrence of uranine in the upper levels compared to bromide and deuterium. There the  
306 modelling results clearly indicated retardation of uranine (Tab. 1). Even though uranine is  
307 generally considered to be a non-sorbing conservative tracer (Käss et al., 1998), as it does not  
308 sorb to negatively charged media such as silica and sandstone, it was found to sorb to  
309 positively charged media such as alumina and carbonate (Kasnavia et al., 1999; Sabatini,  
310 2000). Since the gravel material consisted primarily of silica sand, sorption onto the aquifer  
311 material was not expected. Additionally, uranine is not an ideal tracer in presence of high  
312 organic content (Kasnavia et al., 1999; Smart and Laidlaw, 1977) or salt concentrations  
313 (Magal et al., 2008) which were identified to enhance sorption. Particularly the first may  
314 apply to the investigation site due to presence of brown coal particles in the contaminated  
315 groundwater which were transported and deposited over the years in the gravel bed (Weiss et  
316 al., 1998). This effect was strongest in the middle and upper level of the pilot system where  
317 flow velocities were lowest. In the lower level with high flow velocities, uranine appeared  
318 slightly later and tailing was observed of the BTCs compared to deuterium. This tailing is  
319 likely a consequence of sorption effects, which has also been previously observed in other  
320 wetland systems (Holcová et al., 2013).

321

### 322 **4.3 Evaluation of the wetland performance**

323 The actual residence time in the system is a key factor for evaluating the performance of a  
324 constructed wetland for contaminant removal. Our study shows that tracer studies were

325 necessary to revise results from water balance approaches based on in- and outflow. Unlike  
326 initially assumed, the overall residence time of the groundwater and conservative tracers in  
327 the wetland system (22.0-32.5 d, see Table 2) was lower compared to the theoretical one (34.2  
328 d) resulting in a lower contact and reaction time than previously assumed (Schmidt et al.,  
329 2014). In addition, a preferential flow along the bottom of the wetland system can be  
330 concluded, which is likely due to the constructional design of the inflow resulting in lower  
331 water and contaminant infiltration in the middle and upper levels. Considering mass fluxes in  
332 the wetland, different reactive compartments have to be considered. From a hydrological  
333 point of view the middle and upper layer had 8.6 d and 10.5 d, respectively, longer residence  
334 times compared to the lower level and therefore more potential for reaction and thus, the  
335 removal of contaminants should be higher here. However, lower contaminant mass will be  
336 transported through these regions.

337 To assess the MCB removal efficiency of the model wetland system, MCB concentration  
338 changes during passage in the gravel bed were investigated for the different depths (Figure  
339 S7). There, MCB removal was estimated (see SI) to be 34% in the upper level and 20% in the  
340 middle and lower level, respectively, based on analyzed concentrations only (Table S1).  
341 Highest removal rate and most active zones therefore would supposedly be located in the  
342 upper parts of the wetland. By including the observations from the tracer study our  
343 approximation resulted in similar relative MCB mass removal than estimated above for the  
344 upper and middle layers with 31% and 17%, respectively, while the lower part contributed to  
345 a higher extent with 52% (see Table S1).

346 Based on average oxygen concentrations and redox potentials of the gravel bed ( $0.09 \pm 0.03$   
347  $\text{mg L}^{-1}$ ,  $147 \pm 45$  mV) and especially in the lower level of  $0.08 \pm 0.01$   $\text{mg L}^{-1}$  (Figure S6) and  
348  $108 \pm 22$  mV, respectively, the overall wetland can be considered as anoxic in contrast to the  
349 apparent system analogy and the measured values from Schmidt et al. 2014 (Schmidt et al.,

350 2014). Combining the results, major biological processes driving the MCB removal were  
351 likely anaerobic. The underestimation of MCB degradation in the anoxic zone at the bottom  
352 of the wetland could be only revealed by applying a tracer test combined with the modelling  
353 approach.

354

#### 355 **4.4 Implications for the investigation and implementation of constructed wetlands**

356 Our study stresses the importance of hydrological investigations of constructed wetland as it  
357 can provide valuable insights into water flow, transport and residence times of contaminants  
358 in these systems. The combination of a multi-tracer test with sampling at multiple depths in  
359 the wetland filter, and a mathematical modelling allowed identifying main water flow paths,  
360 variable flow conditions and precise definition of residence times. In our case, the overall  
361 water flow and thus contaminant transport was much faster than expected. Furthermore, the  
362 tracer approach connected with a depth resolved sampling allowed to locate the preferential  
363 flow paths and transport processes. This will help to design and optimize nature-like model  
364 wetland systems for future treatment purposes. The horizontal subsurface flow wetland  
365 system was designed to simulate aquifer-like conditions and to provide as system for  
366 investigation of microbial processes at geochemical gradients. However, in reality the system  
367 turned out to consist of rather heterogeneous flow paths with strongly different transit times  
368 between levels. Consequently, contaminant removal rates were overestimated when only  
369 based on concentration values. Especially, previous assumption of evenly distributed fluxes  
370 and over-estimation of residence times resulted in underestimation of degradation in the lower  
371 level. The contaminant removal efficiency may be improved by altering the wetland design  
372 providing either a more homogeneous flow of groundwater through all parts of the system  
373 with higher reaction times or in an even more heterogeneous flow pattern through different  
374 geochemical zones in the system enhancing gradient based degradation processes. Therefore,

375 for implementation of constructed wetlands as treatment systems, the effect of design  
376 parameters, causing the hydraulic behavior and thus their effect on physical-chemical  
377 parameters, can strongly influence the removal efficiencies of contaminants of the interest  
378 (Kidmose et al., 2010; Onesios et al., 2009). By combining results of multiple conservative  
379 tracers additional information on characteristics such as sorption and flow paths could be  
380 obtained. Overall, even a simple appearing model subsurface flow constructed wetland was  
381 shown to be a complex and heterogeneous system.

382 The HLR in our system was only  $4.8 \text{ mm d}^{-1}$ , which is in the lower range for horizontal  
383 subsurface flow constructed wetlands treating polluted water ( $2\text{-}30 \text{ mm d}^{-1}$ ) (Kadlec and  
384 Wallace, 2008; Wood, 1995). For feasible, commercial, treatment, however, HLR should be  
385 higher, with  $50\text{-}80 \text{ mm d}^{-1}$  (Morel, 2006). Implemented by increasing the inflow rate, an  
386 improved vertical mixing of the treated water and a decrease of the zones of stagnant water  
387 may be accomplished (Headley et al., 2005). Further tests, however, are needed to determine  
388 the limits of the system and maximum loading rates, in concurrence with tracer and  
389 mathematical modeling experiments, to provide a full understanding of the three dimensional  
390 flow and reactive zones within constructed wetland systems.

391

## 392 **5. Conclusions**

393 This work presents the investigation of hydrological flow paths for understanding of the  
394 interactions of biodegradation and transport processes important for remediation approaches  
395 and wetland process based technologies. The design of the constructed wetland basin  
396 determined the flow path, resulting in different zones of stagnant and moving water and  
397 retention times. As a result, contaminants will have different contact times to undergo biotic  
398 or abiotic processes in these zones. In zones of stagnant water the transport of nutrients as  
399 well as electron acceptor and donor, respectively, essential for biotic processes is limited due  
400 to restricted diffusion into these zones. Therefore, degradation reactions might be slower

401 compared to high mobility zones such as at the bottom of the wetland. Especially the  
402 transitions zones between stagnant and mobile water, with related biogeochemical gradients,  
403 are of high interest for an understanding and controlling wetland processes. Overall, this  
404 tracer study combining experimental evaluation with mathematical modeling demonstrated  
405 the complexity of flow and transport processes in the constructed wetlands. This complexity  
406 needs to be taken into account during interpretation of the determining attenuation processes  
407 during treatment of contaminated waters in these engineered systems.

408 **Acknowledgement:**

409 We dedicate this article to the memory of our dear colleague and friend Piotr Maloszewski,  
410 who passed away during the final stages of manuscript preparation. We would like to thank  
411 the Department of Groundwater Remediation, laboratory Bitterfeld, especially Jörg Ahlheim,  
412 Oliver Thiel and Heidrun Paschke for bromide analysis. From the Department of Isotope  
413 Biogeochemistry many thanks to Sameer Devkota, Diana Wolfram, Sascha Lege, Safdar  
414 Bashir, Sara Herrero-Martín and Barbara Klein for volunteering during sampling period and  
415 Falk Bratfisch for D<sub>2</sub>O analysis and Hans-Hermann Richnow for overall support. This study  
416 was funded by the EU FP7 project Genesis (contract number: 226536) and SAFIRA II Project  
417 "Compartment Transfer" (CoTra) of the Helmholtz Centre for Environmental Research –  
418 UFZ.

419

420 **References:**

- 421 Braeckevelt M, Rokadia H, Mirschel G, Weber S, Imfeld G, Stelzer N, et al. Biodegradation  
422 of chlorobenzene in a constructed wetland treating contaminated groundwater. *Water*  
423 *Science and Technology* 2007; 56: 57-62.
- 424 Davis SN, Thompson GM, Bentley HW, Stiles G. Groundwater Tracers - Short Review.  
425 *Ground Water* 1980; 18: 14-23.
- 426 Gambrell RP. Trace and Toxic Metals in Wetlands - a Review. *Journal of Environmental*  
427 *Quality* 1994; 23: 883-891.
- 428 Gearheart R, Klopp F, Allen G. Constructed free surface wetlands to treat and receive  
429 wastewater: pilot project to full scale. *Constructed Wetlands for Wastewater*  
430 *Treatment*. Lewis Publishers, Chelsea, MI 1989: 121-138.
- 431 Gehre M, Strauch G. High-temperature elemental analysis and pyrolysis techniques for stable  
432 isotope analysis. *Rapid Commun Mass Spectrom* 2003; 17: 1497-503.
- 433 Gilley JE, Finkner S, Doran JW, Kottwitz E. Adsorption of bromide tracers onto sediment.  
434 *Applied engineering in agriculture* 1990; 6: 35-38.
- 435 Guo CQ, Cui YL, Dong B, Liu FP. Tracer study of the hydraulic performance of constructed  
436 wetlands planted with three different aquatic plant species. *Ecological Engineering*  
437 2017; 102: 433-442.
- 438 Headley TR, Herity E, Davison L. Treatment at different depths and vertical mixing within a  
439 1-m deep horizontal subsurface-flow wetland. *Ecological Engineering* 2005; 25: 567-  
440 582.
- 441 Hendry MJ, Lawrence JR, Maloszewski P. Effects of velocity on the transport of two bacteria  
442 through saturated sand. *Ground Water* 1999; 37: 103-112.
- 443 Holcová V, Šíma J, Dušek J. A comparison of fluorescein and deuterated water as tracers for  
444 determination of constructed wetland retention time. *Central European Journal of*  
445 *Chemistry* 2013; 11: 200-204.
- 446 Holland JF, Martin JF, Granata T, Bouchard V, Quigley M, Brown L. Effects of wetland  
447 depth and flow rate on residence time distribution characteristics. *Ecological*  
448 *Engineering* 2004; 23: 189-203.
- 449 Imfeld G, Aragonés CE, Fetzer I, Meszaros E, Zeiger S, Nijenhuis I, et al. Characterization of  
450 microbial communities in the aqueous phase of a constructed model wetland treating  
451 1,2-dichloroethene-contaminated groundwater. *Fems Microbiology Ecology* 2010; 72:  
452 74-88.
- 453 Imfeld G, Braeckevelt M, Kusch P, Richnow HH. Monitoring and assessing processes of  
454 organic chemicals removal in constructed wetlands. *Chemosphere* 2009; 74: 349-362.
- 455 Jechalke S, Vogt C, Reiche N, Franchini AG, Borsdorf H, Neu TR, et al. Aerated treatment  
456 pond technology with biofilm promoting mats for the bioremediation of benzene,  
457 MTBE and ammonium contaminated groundwater. *Water Research* 2010; 44: 1785-  
458 1796.
- 459 Kadlec RH, Wallace S. *Treatment Wetlands*, Second Edition: CRC Press, 2008.
- 460 Kaschl A, Vogt C, Uhlig S, Nijenhuis I, Weiss H, Kastner M, et al. Isotopic fractionation  
461 indicates anaerobic monochlorobenzene biodegradation. *Environmental Toxicology*  
462 *and Chemistry* 2005; 24: 1315-1324.
- 463 Kasnavia T, Vu D, Sabatini DA. Fluorescent dye and media properties affecting sorption and  
464 tracer selection. *Ground water* 1999; 37: 376-381.
- 465 Käss W, Behrens H, Himmelsbach T, Hötzl H. *Tracing technique in geohydrology*: Balkema  
466 Rotterdam, 1998.
- 467 Kendall C, McDonnell JJ. *Isotope tracers in catchment hydrology*: Elsevier, 1999.

468 Kidmose J, Dahl M, Engesgaard P, Nilsson B, Christensen BSB, Andersen S, et al.  
469 Experimental and numerical study of the relation between flow paths and fate of a  
470 pesticide in a riparian wetland. *Journal of Hydrology* 2010; 386: 67-79.

471 King AC, Mitchell CA, Howes T. Hydraulic tracer studies in a pilot scale subsurface flow  
472 constructed wetland. *Water Science and Technology* 1997; 35: 189-196.

473 Knorr B, Maloszewski P, Kramer F, Stumpp C. Diffusive mass exchange of non-reactive  
474 substances in dual-porosity porous systems - column experiments under saturated  
475 conditions. *Hydrological Processes* 2016; 30: 914-926.

476 Korom SF. An adsorption isotherm for bromide. *Water Resources Research* 2000; 36: 1969-  
477 1974.

478 Lange J, Schuetz T, Gregoire C, Elsasser D, Schulz R, Passeur E, et al. Multi-tracer  
479 experiments to characterise contaminant mitigation capacities for different types of  
480 artificial wetlands. *International Journal of Environmental Analytical Chemistry* 2011;  
481 91: 768-785.

482 Langergraber G. Modeling of processes in subsurface flow constructed wetlands: A review.  
483 *Vadose Zone Journal* 2008; 7: 830-842.

484 Levy BS, Chambers RM. Bromide as a Conservative Tracer for Soil-Water Studies.  
485 *Hydrological Processes* 1987; 1: 385-389.

486 Li YF, Zhu GB, Ng WJ, Tan SK. A review on removing pharmaceutical contaminants from  
487 wastewater by constructed wetlands: Design, performance and mechanism. *Science of  
488 the Total Environment* 2014; 468: 908-932.

489 Machate T, Noll H, Behrens H, Kettrup A. Degradation of phenanthrene and hydraulic  
490 characteristics in a constructed wetland. *Water Research* 1997; 31: 554-560.

491 Magal E, Weisbrod N, Yakirevich A, Yechieli Y. The use of fluorescent dyes as tracers in  
492 highly saline groundwater. *Journal of Hydrology* 2008; 358: 124-133.

493 Małoszewski P, Wachniew P, Czupryński P. Hydraulic Characteristics of a Wastewater  
494 Treatment Pond Evaluated through Tracer Test and Multi-Flow Mathematical  
495 Approach. *Polish Journal of Environmental Studies* 2006a; 15.

496 Małoszewski P, Wachniew P, Czupryński P. Study of hydraulic parameters in heterogeneous  
497 gravel beds: Constructed wetland in Nowa Słupia (Poland). *Journal of hydrology*  
498 2006b; 331: 630-642.

499 Matamoros V, Bayona JM. Elimination of pharmaceuticals and personal care products in  
500 subsurface flow constructed wetlands. *Environmental Science & Technology* 2006;  
501 40: 5811-5816.

502 Morel A. Greywater management in low and middle-income countries: Dübendorf, CH: Swiss  
503 Federal Institute of Aquatic Science and Technology, 2006.

504 Onesios KM, Yu JT, Bouwer EJ. Biodegradation and removal of pharmaceuticals and  
505 personal care products in treatment systems: a review. *Biodegradation* 2009; 20: 441-  
506 466.

507 Rakoczy J, Remy B, Vogt C, Richnow HH. A Bench-Scale Constructed Wetland As a Model  
508 to Characterize Benzene Biodegradation Processes in Freshwater Wetlands.  
509 *Environmental Science & Technology* 2011; 45: 10036-10044.

510 Ranieri E, Verlicchi P, Young TM. Paracetamol removal in subsurface flow constructed  
511 wetlands. *Journal of Hydrology* 2011; 404: 130-135.

512 Sabatini DA. Sorption and intraparticle diffusion of fluorescent dyes with consolidated  
513 aquifer media. *Groundwater* 2000; 38: 651-656.

514 Schmidt M, Wolfram D, Birkigt J, Ahlheim J, Paschke H, Richnow H-H, et al. Iron oxides  
515 stimulate microbial monochlorobenzene in situ transformation in constructed wetlands  
516 and laboratory systems. *Science of The Total Environment* 2014; 472: 185-193.

517 Smart P, Laidlaw I. An evaluation of some fluorescent dyes for water tracing. *Water  
518 Resources Research* 1977; 13: 15-33.

519 Stump C, Nutzmann G, Maciejewski S, Maloszewski P. A comparative modeling study of a  
520 dual tracer experiment in a large lysimeter under atmospheric conditions. *Journal of*  
521 *Hydrology* 2009; 375: 566-577.

522 Tietz A, Kirschner A, Langergraber G, Sleytr K, Haberl R. Characterisation of microbial  
523 biocoenosis in vertical subsurface flow constructed wetlands. *Science of the Total*  
524 *Environment* 2007; 380: 163-172.

525 Truu M, Juhanson J, Truu J. Microbial biomass, activity and community composition in  
526 constructed wetlands. *Science of the Total Environment* 2009; 407: 3958-3971.

527 Vanderborcht J, Vereecken H. Estimation of local scale dispersion from local breakthrough  
528 curves during a tracer test in a heterogeneous aquifer: the Lagrangian approach.  
529 *Journal of Contaminant Hydrology* 2002; 54: 141-171.

530 Verlicchi P, Zambello E. How efficient are constructed wetlands in removing pharmaceuticals  
531 from untreated and treated urban wastewaters? A review. *Science of the Total*  
532 *Environment* 2014; 470: 1281-1306.

533 Weis JS, Weis P. Metal uptake, transport and release by wetland plants: implications for  
534 phytoremediation and restoration. *Environment international* 2004; 30: 685-700.

535 Weiss H, Daus B, Fritz P, Kopinke F-D, Popp P, Wuensche L. In situ groundwater  
536 remediation research in the Bitterfeld region in eastern Germany (SAFIRA). IAHS  
537 Publication(International Association of Hydrological Sciences) 1998: 443-450.

538 Whitmer S, Baker L, Wass R. Loss of bromide in a wetland tracer experiment. *Journal of*  
539 *Environmental Quality* 2000; 29: 2043-2045.

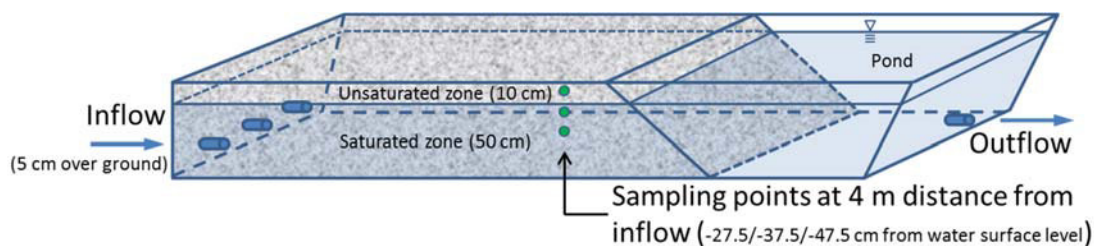
540 Wood A. Constructed wetlands in water pollution control: Fundamentals to their  
541 understanding. *Water Science and Technology* 1995; 32: 21-29.

542 Zahraeifard V, Deng ZQ. Hydraulic residence time computation for constructed wetland  
543 design. *Ecological Engineering* 2011; 37: 2087-2091.

544

545

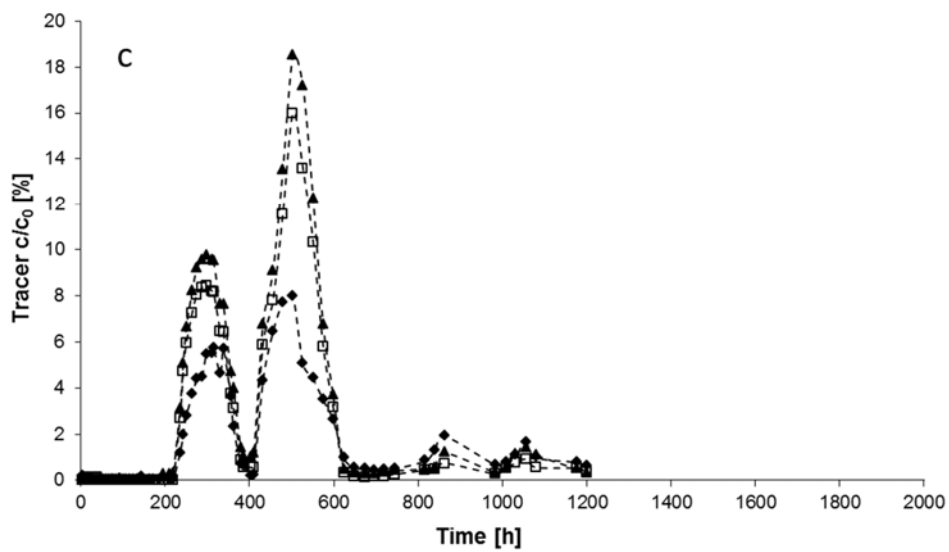
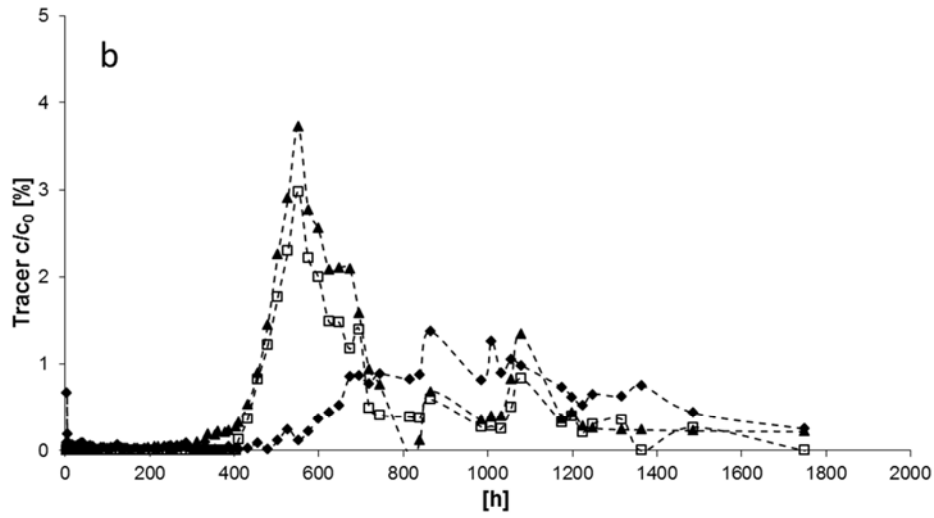
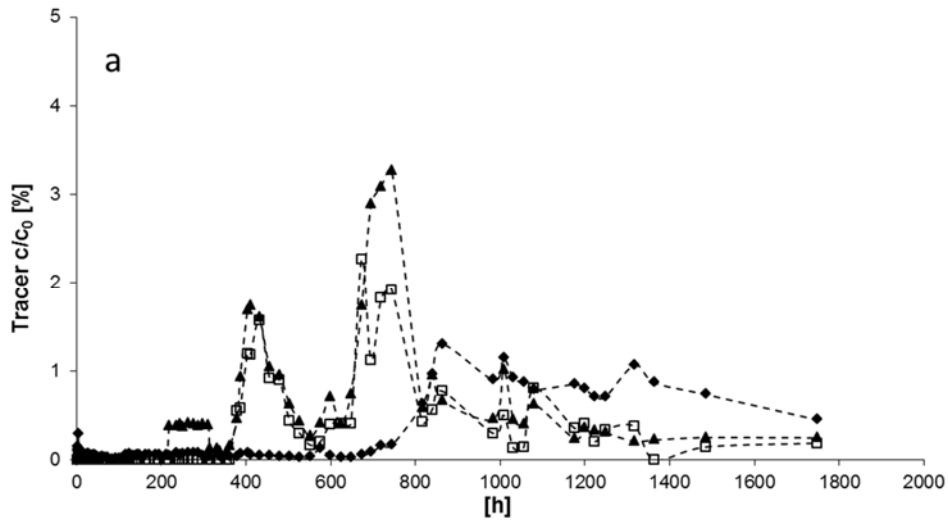
546 **Figures:**



547

548 **Figure 1.** Schematic model of the constructed wetland system in Bitterfeld with the  
549 dimension of 6 m (length) x 1 m (width) x 0.6 m (depth) consisted of a gravel bed (5 m x 1 m  
550 x 0.6 m) and a free water pond (1 m x 1 m x 0.5 m) at the outflow side. Green dots represent  
551 the sampling points in 4 m after the inflow in direction of flow in three different depths (-27.5

552 cm; -37.5 cm; -47.5 cm from water surface level). Injection of tracer solution was done at  
553 decoupled inflow pump via a 40 L stainless steel tank.



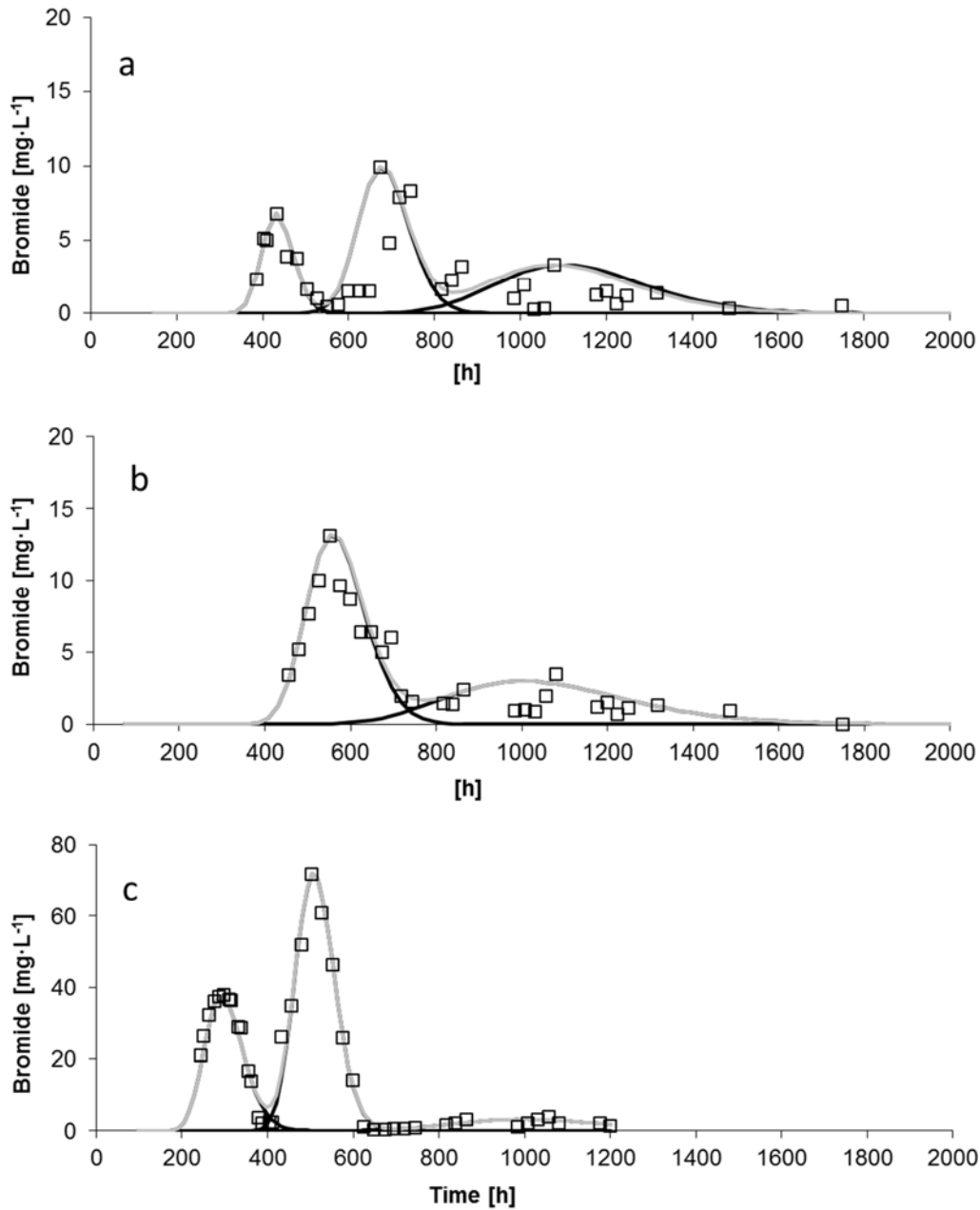
555 **Figure 2.** Results of breakthrough curves of the tracers deuterium ( $\blacktriangle$ ), bromide ( $\square$ ) and  
556 uranine ( $\blacklozenge$ ) at 4 m from inflow in the sampled depths. Response of tracer concentrations  
557 normalized to the initial concentrations ( $c/c_0$ ) over time after pulse injection in the upper level  
558 (a), middle level (b) and lower level (c), respectively.

559

560

561

562



563

564 **Figure 3.** Calibration the MFDM to bromide concentration over time after pulse injection in  
 565 the different levels at  $z = -27.5$  cm (a),  $z = -37.5$  cm (b) and  $z = -47.5$  cm (c), respectively at  $x$   
 566  $= 4$  m. Observed sampled bromide concentrations ( $\square$ ) and fitted RTD curves obtained with the  
 567 MFDM of each breakthrough curve (black lines) and complete tracer regime (grey line).

568

569 **Table 1.** Overview of parameters derived from the MFDM of all tracers and different sampled levels at 4 m horizontal distance from inflow where  
 570 T represents the transit time, v the velocity,  $\alpha_L$  the longitudinal dispersivity and p the portion of tracer mass.

		Lower level Depth z = -47.5 cm			Middle level Depth z = -37.5 cm			Upper level Depth z = -27.5 cm		
		Deuterium	Bromide	Uranine	Deuterium	Bromide	Uranine	Deuterium	Bromide	Uranine
Curve 1										
	T [d]	12.7	12.6	12.6	24.1	23.8	32.0	18.0	18.2	40.8
	v [m d <sup>-1</sup> ]	0.32	0.32	0.32	0.17	0.17	0.13	0.22	0.22	0.10
	$\alpha_L$ [cm]	4.6	4.6	3.8	3.6	2.9	7.0	1.5	1.4	4.0
	p [-]	0.30	0.29	0.31	0.78	0.59	0.49	0.22	0.18	0.47
Curve 2										
	T [d]	21.4	21.4	20.1	46.0	44.5	46.0	30.4	28.6	59.7
	v [m d <sup>-1</sup> ]	0.19	0.19	0.20	0.09	0.09	0.09	0.13	0.14	0.07
	$\alpha_L$ [cm]	1.6	1.6	2.2	0.5	8.3	3.5	1.0	1.5	3.0
	p [-]	0.57	0.54	0.49	0.22	0.41	0.28	0.48	0.42	0.53
Curve 3										
	T [d]	41.2	43.5	40.0	-	-	61.5	41.7	46.5	-
	v [m d <sup>-1</sup> ]	0.10	0.09	0.10	-	-	0.07	0.10	0.09	-
	$\alpha_L$ [cm]	4.0	6.4	4.3	-	-	2.0	2.8	5.0	-
	p [-]	0.13	0.17	0.20	-	-	0.23	0.30	0.40	-

Weighted mean transit time	T [d]	21.4	22.6	21.8	28.9	32.3	42.7	31.1	33.9	50.8
-------------------------------	-------	------	------	------	------	------	------	------	------	------

571

572

573 **Table 2.** Calculated relative portions of tracer mass of two ideal tracers (deuterium, bromide)  
 574 and mean values of flux portion, transit time and volume of active water in the different levels  
 575 derived from the MFDm.

Level	Portion of whole tracer mass $p_j$ [-]		Mean portion of tracer mass	Mean transit time	Mean volume of active water
	Deuterium	Bromide	$p_{j \text{ mean}}$ [-]	$T_{j \text{ mean}}$ [d]	$V_{j \text{ mean}}$ [m <sup>3</sup> ]
Lower (-47.5 cm)	0.70	0.65	0.68	22.0	0.36
Middle (-37.5 cm)	0.14	0.18	0.16	30.6	0.12
Upper (-27.5 cm)	0.16	0.17	0.16	32.5	0.13

576